

Document downloaded from:

<http://hdl.handle.net/10251/67998>

This paper must be cited as:

Betoret Valls, ME.; Betoret Valls, N.; Castagnini, JM.; Rocculi, P.; Dalla Rosa, M.; Fito Maupoey, P. (2015). Analysis by non-linear irreversible thermodynamics of compositional and structural changes occurred during air drying of vacuum impregnated apple (cv. Granny smith). Calcium and trehalose effects. *Journal of Food Engineering*. 147:95-101. doi:10.1016/j.jfoodeng.2014.09.028.



The final publication is available at

<https://dx.doi.org/10.1016/j.jfoodeng.2014.09.028>

Copyright Elsevier

Additional Information

1 **Analysis by non-linear irreversible thermodynamics of**
2 **compositional and structural changes occurred during air**
3 **drying of vacuum impregnated apple (cv. *Granny smith*):**
4 **calcium and trehalose effects.**

5

6 E. Betoret^{a*}, N. Betoret^b, J.M. Castagnini^b, P. Rocculi^a, M. Dalla Rosa^a, P. Fito^b.

7 ^aDipartimento di Scienze e Tecnologie Agro-Alimentari, Alma Mater Studiorum
8 Università di Bologna, Piazza Goidanich 60, 47023 Cesena, Italy.

9 ^bInstitute of Food Engineering for Development, Department of Food
10 Technology, Universitat Politècnica de València, Camino de Vera s/n, 46022
11 Valencia, Spain.

12

13 * Corresponding author: Dipartimento di Scienze e Tecnologie Agro-Alimentari, Alma Mater
14 Studiorum Università di Bologna, Piazza Goidanich 60, 47023 Cesena, Italy. Tel: +39 0547
15 338120 Fax: +39 0547 382348. e-mail address: maria.betoretvalls@unibo.it (E. Betoret)

16

17

18 **Abstract**

19 Apple discs were impregnated with isotonic solutions of sucrose and trehalose with and
20 without calcium addition and after air dried. In the vacuum impregnation experiments,
21 the calcium and the replacement of sucrose by trehalose did not have significant effect
22 on the final volumetric deformation of the samples. During air drying two stages of
23 changes were considered. The first one lasted until the saturation of the intracellular
24 liquid phase, and the second one from the saturation of the intracellular liquid phase
25 until the end of the drying process. Mass transfer has been analysed applying
26 nonlinear irreversible thermodynamics. Water flux, water chemical potential and tissue
27 shrinkage have been taken into account in order to accurately describe the mass

28 transfer phenomena during air drying. A precise definition of chemical potential allowed
 29 estimating the partial molar energy needed for breakages and the reversible and
 30 irreversible deformations of tissue structure coupled with mass transfer during air
 31 drying of apple.

32 **Keywords:** *apple, drying modelling, vacuum impregnation, calcium, trehalose*

33

34 **NOMENCLATURE**

Suc	sucrose	
Tre	trehalose	
Ca	calcium	
s.d.	standard deviation	
a	activity	
w	water	
VI	vacuum impregnation	
w.b.	wet basis	
d.b.	dry basis	
X	volumetric fraction of exchanged liquid	$m^3_{\text{exchanged liquid}}/m^3_{\text{total}}$
x	mass fraction	$kg_{\text{component}}/kg_{\text{total}}$
V	volume	m^3
V'	partial molar volume	m^3/mol
m	weight	kg
S	area of the interface solid-air	m^2
J	flux	$\text{mol}/m^2 \cdot s$
L	phenomenological coefficient	$\text{mol}^2/\text{J} \cdot m^2$
Mr	molecular weight	kg/mol
t	time	s
T	temperature	K
R	ideal gases constant	J/mol·K
P	pressure	N/m ²
Greek symbols		
μ	chemical potential	J/mol
φ	relative humidity of the air in contact with the fruit	

ρ	density	kg/m^3
ϵ	porosity	$\text{m}^3_{\text{internal gas}}/\text{m}^3_{\text{sample}}$
γ	volumetric deformation	$\text{m}^3_{\text{volume variation}}/\text{m}^3_{\text{total}}$

Subscripts

pi	impregnated product
ml	liquid medium
pf	fresh product
1	at the end of the vacuum stage
e	effective
Ca	calcium
w	water
int	internal
ext	external
O	initial
S	saturation
DE	deformation
R	breakage

Superscripts

cal	calculated
------------	------------

35

36 1. INTRODUCTION

37 In the most part of the studies about food dehydration by hot air, it is accepted
38 that diffusion is the only mechanism implicated in water flux and the operation is
39 modelled using Fick's equations deduced for ideal gas systems (Bolin &
40 Stafford, 1974; El Halouat & Labuza, 1987; Senhaji *et al.*, 1991; Sabarez &
41 Price, 1999; Yang *et al.*, 2001). In other research papers the transport
42 phenomena are described with coefficients estimated from semi-empirical
43 correlations and referred to samples having a constant and specific dimension.
44 When food shape is not regular (i.e. shrinkage is significant) this approach
45 might significantly limits the model accuracy, providing unreliable predictions of

46 the system behaviour (Bernstein & Noreña, 2013). Nowadays, there are
47 complex models that analyse the dehydration process by microscopy studies,
48 accounting for heat and mass transfer in the different food phases. In most
49 cases, for their application, these models need parameters that are impossible
50 to obtain experimentally (Ratti, 2001). A lot of efforts have been made trying to
51 model convective drying of food products considering the samples shrinkage
52 (Kowalski, 1996; Hernández *et al.*, 2000; Márquez & De Michelis, 2011; Aversa
53 *et al.*, 2012; Curcio & Aversa, 2014). Shrinkage affects the predictions of both
54 moisture and temperature profiles (Mayor & Sereno, 2004) and it has
55 necessarily to be taken into account when a mathematical model aimed at
56 describing drying process is being formulated (Márquez & De Michelis, 2011).
57 The SAFES methodology (Systematic Approach to Food Engineering Systems)
58 is an advanced method to analyse food products and processes (Fito *et al.*,
59 2007). With this method, it is possible to describe products taking into account
60 thermodynamics, physicochemical and structural characteristics and to analyse
61 the changes (i.e. transport phenomena, phase transitions, structural changes...)
62 produced in food by basic operation or transformation phenomena in a
63 systematic way (Fito *et al.*, 2007; Barrera *et al.*, 2007; Betoret *et al.*, 2007).
64 In polyphasic, multicomponent and structured dried foods, the structure and the
65 structural modifications, suffered by the product during the process, induce
66 fluxes promoted by non diffusional mechanisms from driving forces different to
67 the concentration gradients (Barat *et al.*, 2001). Different studies have shown
68 that water transport coupled with deformation-relaxation phenomena have big
69 influence on this aspect (Barat *et al.*, 1998; Fito *et al.*, 1996). Actually, the
70 incorporation into the product of any components that can affect mechanical

71 properties of the structure could have influence on the dehydration process
72 kinetics. The irreversible deformation caused to the dried samples strongly
73 damages the cellular tissue, resulting in low quality dehydrated products. Some
74 studies confirm the interaction and the effect of the calcium and the trehalose
75 on the structural characteristics of different fruits (Gras *et al.*, 2003; Barrera *et*
76 *al.*, 2004; Barrera *et al.*, 2009; Jain *et al.*, 2009; Paik *et al.*, 2005). These
77 compounds could help to control the deformation, increasing the quality of the
78 final product.

79 The aim of this work is to determine the calcium and the trehalose effects on the
80 volumetric deformation of apple disc samples and on the tissue shrinkage
81 during drying, when these elements are incorporated into the tissue by vacuum
82 impregnation. The investigation has been also performed analysing the mass
83 transfer kinetics and the deformation-relaxation phenomena by non linear
84 irreversible thermodynamics.

85

86 **2. MATERIALS AND METHODS**

87 Experiments were carried out using apples (var. *Granny Smith*) purchased from
88 local market. Fruits were cut into disc-shaped samples 5 mm thick, following
89 their vertical axis. The apple skin and seeds were removed with two cylinders.
90 The internal diameter of the samples was 20.7 mm and the external one 64.4
91 mm. From each fruit five discs were obtained: four were vacuum impregnated
92 with sucrose, sucrose-calcium, trehalose and trehalose-calcium solutions and
93 the fifth was used to determine humidity content and refraction index.
94 Impregnated discs were cut in half: one part was dried using hot air at 40 °C

95 and the other one was used to determine humidity content, refraction index and
96 water activity.

97 To impregnate apple samples, four aqueous solutions with sucrose, trehalose,
98 sucrose and calcium and trehalose and calcium were used. The composition of
99 the solutions was calculated in order to be isotonic with the apple tissue.

100

101 2.1. Humidity content, water activity and refraction index.

102 The humidity content was determined following the official method 20.013
103 (AOAC, 1980) for dried fruits with high sugar content.

104 The water activity was determined with a dew point hygrometer mod. Aqualab
105 CX-2 (Decagon Devices Inc., Pullman, WA) calibrated previously with saturated
106 reference solutions.

107 The refraction index was determined with a thermostated refractometer mod.
108 Pal-1 (ABBE ATAGO Co., Tokyo, Japan).

109

110 2.2. Vacuum impregnation.

111 VI operation was carried out with a pilot plant equipment developed in the
112 Department of Food Technology at Polytechnic University of Valencia (Fito *et*
113 *al.*, 1996).

114 In the vacuum experiments, the sample was immersed in the impregnation
115 solution. A vacuum pressure of 50 mbar was applied for 10 min, and then
116 atmospheric pressure was restored leaving samples immersed in the liquid for
117 an additional period of 10 min.

118 To determine the impregnation properties of the apple tissue, the experimental
119 methodology developed by Salvatori *et al.* (1998) was followed. Salvatori *et al.*,

120 in (1998) established a general procedure to evaluate the feasibility of VI by
121 determining deformation and impregnation level in the product. In this
122 procedure the samples and the impregnation liquid are weighted at different
123 moments during an experimental vacuum impregnation operation.

124

125 2.3. Hot air drying.

126 Hot air drying operation was carried out with a pilot plant equipment developed
127 in the Department of Food Technology at Polytechnic University of Valencia
128 (Martín, 2002).

129 Four samples from the same apple, impregnated with sucrose, sucrose-
130 calcium, trehalose and trehalose-calcium solutions, were air dried
131 simultaneously during 900 min. Temperature (40 ± 0.03) °C and relative
132 humidity of the air (56 ± 2.01) were monitored by a computer during all period.
133 In all the experiments, the flow rate was maintained at $3.7 \text{ kg wet air/m}^2\cdot\text{s}$.

134 The initial humidity of the samples was determined then the samples were
135 weighed (mod. PB303-S, Mettler Toledo Inc., Barcelona, Spain), thickness
136 measured and their images area acquired (mod. D400, Nikon, Barcelona,
137 Spain), all parameters were determined during all the drying process, every 5
138 min during the first 15 min, at 15 min intervals until one hour of drying, at 30 min
139 intervals until two hours of drying and 1 hour interval until the end of the drying
140 process. Using digitalized images the area of the interface solid-air was
141 estimated by image analysis using the software Photoshop v.7.0 (Adobe
142 Systems Incorporated, USA).

143

144 2.4. Statistical analysis.

145 All the values provided are the average of at least three replicates and to
146 determine the significant differences of the results the analysis of variance test
147 was carried out (One-way ANOVA or Multifactor ANOVA) with confidence level
148 of 95 % ($p < 0.5$) using the program STATGRAPHICS PLUS v.5.1.

149

150 3. RESULTS AND DISCUSSION

151 3.1. Vacuum impregnation: Effect of the different solutes on volumetric
152 deformation of the samples at the end of the vacuum impregnation
153 process.

154 According to the hydrodynamic mechanism model described by Salvatori *et al.*,
155 (1998) and using the weight of the sample registered during the vacuum
156 impregnation experiment, it was possible to determine the impregnation
157 parameters at the end of the vacuum period ($X_1, \gamma_1, \varepsilon_1$) and also at the end of
158 the vacuum impregnated process (X, γ, ε) (Fito *et al.*, 1996; Salvatori *et al.*,
159 1998). In table 2, the average values and standard deviations of these
160 parameters are shown for the apple samples impregnated with the different
161 solutions.

162 The impregnation volumetric value of the samples (X) can be used in mass
163 balance equation (eq. 1) (Fito *et al.*, 2000) to determine the mass fraction of
164 sugar and calcium that are incorporated into the samples for each case.

165

$$X_{pi} = \frac{X_{ml} X \frac{\rho_{ml}}{\rho_{pf}} + X_{pf}}{1 + X \frac{\rho_{ml}}{\rho_{pf}}} \quad (1)$$

166 In previous studies it has been proved that impregnation and deformation
167 phenomena are coupled (Fito *et al.*, 1996; Salvatori *et al.*, 1998). For similar

168 values of effective porosity (ϵ_e), a decreasing of X value is followed by an
169 increasing in the volumetric deformation of the sample. In the same previous
170 studies, negative values of X_1 have been related with an exit of the native liquid
171 from intercellular spaces of the fresh tissue.

172 Protective aspects of trehalose in cellular structures (Miller *et al.*, 1997) and
173 membranes (Crowe & Crowe, 1992) might produce an effect in the fruit tissue
174 affecting the impregnation parameters. In the same way, different studies with
175 vegetal tissue impregnated with calcium in different concentration level (Gras *et*
176 *al.*, 2001; Salvatori *et al.*, 2011) have shown that when the calcium content
177 exceed a concentration level of 10 g/L produces a modification in the elastic
178 properties of the structure, and a bigger volumetric deformation of the samples
179 (Betoret *et al.*, 2003). The coupling of the hydrodynamic mechanism with
180 deformation-relaxation phenomena in the solid matrix of the food explains a
181 modification in the elastic properties of the structure at different impregnation
182 levels. Nevertheless, a multiple analysis of variance showed, with a confidence
183 level of 95 % that the presence of calcium and the replacement of sucrose by
184 trehalose did not have a significant effect on the impregnation and volumetric
185 deformation of the samples at the end of the process. In our case it seems that
186 the samples have not reached the calcium or trehalose content needed to affect
187 food structures during VI operation.

188

189 3.2. Dehydration operation: determination of the critical point and
190 modelling.

191 After the VI with the different solutions, apple discs were air dried. Mass and
192 volume variation of the samples were determined during the whole drying

193 process. In figure 1 the values of the variables: humidity (w.b) (x_w) ($\text{kg}_w/\text{kg}_{\text{product}}$),
194 humidity (d.b) referred to the initial value (x_w/x_{w0}), volume referred to the initial
195 value (V/V_0), water flux (J_w) ($\text{mol}/\text{m}^2\cdot\text{s}$) and chemical potential ($RT\ln a_w/\varphi$)
196 (J/mol) versus treatment time for each impregnation solution are reported.

197 Around 200 min of drying, a critical point was identified. At this moment, the
198 liquid phase of the samples becomes saturated (t_s). The determination of the
199 saturation time was established considering the saturation point of an aqueous
200 liquid phase with sucrose and trehalose at 40 °C. Taking into account the
201 solutes concentration of intra and extracellular liquid phases and the water
202 content of the sample, it was possible to establish the specific drying time in
203 which the liquid phase becomes saturated (Table 3).

204 At this point, the sample has lost the 70 % of the initial volume (about 82 % at
205 the end of the process). Furthermore, until this moment, the volume loss has
206 been proportional to the humidity loss (d.b) and to the volume loss of the liquid
207 phase. From this point, there was a short period of time (until 300 min) where
208 the product continues losing humidity faster than volume (Figure 2). Finally,
209 from 350 - 400 min the volume did not change and the rest of the variables
210 decreased very slowly.

211 During the first drying stage, the sample, previously impregnated with the
212 different solutions, is in contact with hot air that has a lower water activity than
213 the fruit tissue. The loss of water from the surface of the fruit produces water
214 chemical potential gradients. The liquid water migrates towards surface by
215 different mechanisms (i.e. apoplastic, symplastic, transmembrane (active and
216 osmotic), diffusive on the liquid phase of the intercellular space...). In all cases,
217 water spontaneous transport towards surfaces consumes free energy. The

218 driving forces that promote this spontaneous transport are based in gradients of
219 intensive state variables (pressure, temperature or concentration, in this last
220 case using chemical potential function). Free energy consumed for water
221 transport, at constant pressure and temperature, can be calculated from the
222 difference between the chemical potential inside and outside the fruit tissue (2):
223

$$\Delta\mu_w = RT \ln \frac{\Delta\mu_{wint}}{\Delta\mu_{wext}} = RT \ln \frac{a_w}{\phi} \quad (2)$$

224
225 When different pressures inside and outside the fruit tissue exist (for example,
226 in the case of turgor existence) the equation 2 is transformed into:
227

$$\Delta\mu_w = RT \ln \frac{a_w}{\phi} + V'_w (P_{int} - P_{ext}) \quad (3)$$

228
229 When the pressure term is positive (for example in the case of turgor existence)
230 the equation 3 indicates the existence of “free additional energy” available for
231 water transport (Fito *et al.*, 2007).

232 The chemical potential described as above keeps the physical meaning: the
233 partial molar free energy available for the spontaneous water transport between
234 two points of the system.

235 Sometimes, this water transport can be conditioned to the necessary
236 modification/generation of the structures with the “additional consumption” of
237 the available free energy for the transport (Fito *et al.*, 2007). In this case,
238 equation 3 is transformed into:

239

$$\Delta\mu_w = RT \ln \frac{a_w}{\phi} + V'_w (P_{\text{int}} - P_{\text{ext}}) - V'_w (\Delta P_{\text{DE}} - \Delta P_{\text{R}}) \quad (4)$$

240

241 The equation 4 indicates that the molar free energy available for the mass
242 transport has been reduced by the third term of the equation. The third term of
243 the right side of equation evaluates the molar energy used in the elastic and
244 reversible deformation of the structures ($V'_w \cdot \Delta P_{\text{DE}}$) and the dissipated energy in
245 breakages and/or irreversible deformations ($V'_w \cdot \Delta P_{\text{R}}$). The physical meaning of
246 the terms ΔP_{DE} and ΔP_{R} is: the pressure increments needed to produce elastic
247 deformation and breakages or irreversible deformations respectively or the
248 internal mechanic effort that it is used to modify/generate structures. The energy
249 consumption decreases the water flux that could be possible with the same
250 gradient of chemical potential calculated with equation 2.

251 The coupling between the different phenomena and the mechanisms of mass
252 and energy transport are common during the cellular systems drying (Barat *et al.*,
253 2001). The water losses necessarily involve the decrease of the protoplast
254 volume and consequently the membrane and the wall are deformed or
255 completely separated (microscopic level) (Seguí *et al.*, 2006). The structural
256 changes produced at microscopic level result at macroscopic level with the
257 change of the general aspect of the sample or shrinking and with important
258 modifications in the physicochemical properties during the stage.

259 Taking into account the above considerations and the non linear irreversible
260 thermodynamics, the water flux from inside the product towards drying air can
261 be calculated by the equation 5 and also quantified by phenomenological
262 equation (Seguí *et al.*, 2006):

263

$$J_w = \frac{1}{S \cdot M r_w} \frac{\Delta(m \cdot x_w)}{\Delta t} \quad (5)$$

264

$$L_w = \frac{J_w}{\Delta \mu_w} \quad (6)$$

265

266 Taking into account equation 4:

267

$$L_w = \frac{J_w}{RT \ln \frac{a_w}{\phi} + V'_w (P_{int} - P_{ext}) - V'_w (\Delta P_{DE} - \Delta P_R)} \quad (7)$$

268

269 Experimental data obtained in this work allowed calculating the first term of the
 270 right side of equation 4. The value of the phenomenological calculated
 271 coefficient results:

272

$$L_w^{cal} = \frac{J_w}{RT \ln \frac{a_w}{\phi}} \quad (8)$$

273

274 The physical meaning of phenomenological coefficient is: a measure of how the
 275 driving force gradient can contribute to the water transport. It is possible to
 276 predict the second term of right side of equation 4 that can be only a positive
 277 value (increasing the driving force) during the first minutes of drying. A small
 278 loss of water implicates, in all cases, a turgor loss and therefore the term
 279 becomes zero.

280 When deformation-relaxation phenomena exist the third term of the right side of
 281 equation 4 will be negative (depending on the volume increase of the sample in

282 each moment) (Fito *et al.*, 2007). If there is not turgor or related to water
283 transport:

284

$$L_w^{cal} = L_w \quad (9)$$

285

286 When the turgor or deformation-relaxation phenomena exist:

287

Fruit with turgor: $L_w^{cal} \geq L_w \quad (10)$

Deformations: $L_w^{cal} \leq L_w \quad (11)$

288

289 In the figures 3 and 4 the values of the water flux and phenomenological
290 coefficient, calculated without consider turgor and deformation effects, are
291 represented.

292 At initial drying stages there is a substantial flux of water from the sample to the
293 drying air. However the chemical potential remains constant. The loss of free
294 water present in the intercellular spaces or pores of the tissue in a product with
295 high moisture content scarcely affects water activity and thereof the chemical
296 potential considered. Then, the water flux is accompanied by a proportional
297 decrease in the chemical potential. During this period the liquid intracellular
298 water is eliminated reducing the water activity of the product. Finally the water
299 strongly linked to the tissue is eliminated. In this period the deformation-
300 relaxation phenomena are very important. Small water fluxes are followed by
301 significant variations in the water activity of the tissue and consequently in the
302 chemical potential considered.

303 After 10 minutes of drying (when deformation is not excessive) it can be
304 supposed that L_w calculated is close to the real. Assuming this real value, the
305 difference between real and calculated L_w allow us to calculate structural
306 deformation efforts.

307

$$V'_w(\Delta P_{DE} + \Delta P_R) = \left(\frac{1}{L_w} - \frac{1}{L_w^{cal}} \right) J_w \quad (12)$$

308

309 Evolution of the free energy to generate structural deformation/breakages
310 efforts versus time is represented in the figure 5.

311 The elastic response of plant tissues has been attributed to cellulose, the main
312 component of the cell wall, which provides individual cells with rigidity and
313 resistance to rupture (John & Dey, 1986; Pitt, 1992); to the occluded air in the
314 porous matrix and; to the turgor pressure which leads to the rigidity of plant cells
315 and tissues, and, together with the cell wall, provides the mechanical support for
316 maintaining cell and tissue shape (Bourne, 1976; Alzamora *et al.*, 2000). The
317 presence of calcium in the wall matrix can help to maintain middle lamella
318 integrity, since it promotes cross-linking of pectin polymers, and in addition can
319 make pectin macromolecules of the cell wall less soluble through the formation
320 of bridges between them (Salvatori *et al.*, 2011). This fact has been related with
321 increasing the stiffness and fragility of the cellular network (Gras *et al.*, 2003). In
322 our case, the free energy used for breakages and irreversible deformations is
323 not affected in a general way by calcium. In the samples Tre and Tre+Ca the
324 curves obtained are overlapped; however in the samples Sac and Sac+Ca it is
325 possible to see, at the end of the drying process, a tendency to increase the
326 deformations efforts in the samples impregnated with calcium.

327 Regarding to sugar treatment, previous work has shown that non-reducing
328 disaccharides such as sucrose and trehalose can protect biological systems
329 from the adverse effects of freezing and drying (European Patent Application,
330 1999; Aktas *et al.*, 2007). Trehalose has been claimed to be a desiccation
331 protectant (Miller *et al.*, 1997; Ferrando & Spiess, 2001), suggesting that the
332 use of this sugar could result in an improved preservation of plant cellular
333 structure. Atarés *et al.*, (2008) found that apple cylinders osmotically dehydrated
334 with trehalose showed a better solute retention during rehydration, an indicator
335 of the cellular disruption suffered by the material. The ability to form glasses and
336 direct interaction between the sugar and polar groups in proteins and
337 phospholipids would be responsible for stabilization. In our case, it is possible to
338 see clearly the differences between trehalose and sucrose on the evolution of
339 the free energy to generate structural deformations/breakages. After the critical
340 point (200 min drying), when the liquid phase becomes saturated, there is a
341 tendency change between both sugars. The free energy in Sac and Sac+Ca
342 samples decreases abruptly which means the progressive failure of the cellular
343 structure. However the free energy in Tre and Tre+ca samples is maintained
344 until the end of drying, showing a bigger deformation capacity of the samples
345 thus preventing the cellular disruption and breakages. As tissues are dried,
346 hydrogen bonding between trehalose and the polar lipids of biomembranes has
347 been demonstrated to replace the water of hydration at the membrane-fluid
348 interface, preventing the phase transition from lamella to gel phase and the
349 consequent leakage (Nieto *et al.*, 2013).

350

351 **4. CONCLUSIONS**

352 According to obtained results the calcium had not effect on volumetric
353 deformation of samples after vacuum impregnation neither hot air drying. Air
354 drying operation analysis by non linear irreversible thermodynamics allowed
355 calculating the free energy to generate structural deformation/breakages efforts
356 during the drying time for all the samples. The replacement of sucrose by
357 trehalose had significant effect during drying.

358 The calculations obtained showed bigger free energy related with structural
359 efforts in the samples impregnated with trehalose, an indicator of cellular
360 structure maintenance.

361

362 **ACKNOWLEDGEMENTS**

363 The authors thank the Spanish Government (Ministerio de Ciencia e Innovación) for
364 financial support to the project AGL2009-09905. The authors also acknowledge the
365 European Commission for its contribution throughout the FoodSPProcess project.

366

367 **REFERENCES**

- 368 A.O.A.C., (1980). Association of official analytical chemist. *Official Methods of Analysis*,
369 20013. Washington, D.C.
- 370 Aktas, T., Fujii, S., Kawano, Y., & Yamamoto, S. (2007). Effects of pretreatments of
371 sliced vegetables with trehalose on drying characteristics and quality of dried
372 products. *Food and Bioproducts Processing*, 85(C3), 178-183.
- 373 Alzamora, S.M., Castro, M.A., Nieto, A.B., Vidales, S.L., & Salvatori, D.M. (2000) The
374 role of tissue microstructure in the textural characteristics of minimally processed
375 fruits. In: *Minimally processed fruits and vegetables*, Alzamora, S.M., Tapia, M.S., &
376 López-Malo, A. (eds), Aspen Publishers Inc., Gaithersburg, 153-171.

377 Atarés, L., Chiralt, A., & González-Martínez, C. (2008). Effect of solute on osmotic
378 dehydration and rehydration of vacuum impregnation impregnated apple cylinders
379 (cv. Granny Smith). *Journal of Food Engineering*, 89, 49-56.

380 Aversa, M., Curcio, S., Calabrò, V., Iorio, G. (2012) Experimental evaluation of quality
381 parameters during drying of carrot samples. *Food and Bioprocess Technology*, 5,
382 118–129.

383 Barat, J. M., Chiralt, A., & Fito, P. (1998). Equilibrium in cellular food osmotic solution
384 systems as related to structure. *Journal of Food Science*, 63(5), 836–840.

385 Barat, J.M., Fito, P., Chiralt, A. 2001. Modelling of simultaneous mass transfer and
386 structural changes in fruit tissues. *Journal of Food Engineering*, 49 (23): 77-85.

387 Barrera, C., Betoret, N., & Fito P. (2004) Ca²⁺ and Fe²⁺ influence on the osmotic
388 dehydration kinetics of apple slices (var. Granny Smith). *Journal of Food*
389 *Engineering*, 64, 9-14.

390 Barrera, C., Betoret, N., Heredia, A., Fito, P. (2007) Application of SAFES (Systematic
391 Approach to Food Engineering Systems) methodology to apple candying, *Journal of*
392 *Food Engineering*, 83, 193-200.

393 Barrera, C., Betoret, N., Corell, P., & Fito P. (2009) Effect of osmotic dehydration on the
394 stabilization of calcium-fortified apple slices (var. Granny Smith): Influence of
395 operating variables on process kinetics and compositional changes. *Journal of Food*
396 *Engineering*, 92, 416–424

397 Bernstein, A., Noreña, C.P.Z., 2013. Study of thermodynamic, structural, and quality
398 properties of yacon (*Smallanthus sonchifolius*) during drying. *Food and Bioprocess*
399 *Technology*. <http://dx.doi.org/10.1007/s11947-012-1027-y>.

400 Betoret, N., Martínez-Monzó, J., Fito, P.J., Fito, P. (2003). Calcium and iron distribution
401 in fortified vacuum impregnated fruits determined by EDX-Ray Microanálisis. *Journal*
402 *of Food Science*, January/February 2005, Vol. 70, Nr. 1.

403 Betoret, N., Andrés, A., Seguí, L., Fito, P. (2007) Application of safes (systematic
404 approach to food engineering systems) methodology to dehydration of apple by
405 combined methods, *Journal of Food Engineering*, 83, 186-192.

406 Bolin, H.R. & Stafford, A.E. (1974). Effects of processing and storage on provitamin A
407 and vitamin C in apricots. *Journal of Food Science*, 39, 1034–1036.

408 Bourne, M.C. (1976) Texture of fruits and vegetables. In: *Rheology and Texture in Food*
409 *Quality*, DeMan, J.M., Voisey, P.W., Rasper, V.F., & Stanley, D.W. (eds), Van
410 Nostrand Reinhold/AVI, New York, 275-307.

411 Crowe, L.M. & Crowe, J.H. (1982) Hydration – dependent hexagonal phase in a
412 biological membrane. *Archives of Biochemistry and Biophysics*, 769, 141-150.

413 Curcio, M. & Aversa, S. (2014) Influence of shrinkage on convective drying of fresh
414 vegetables: A theoretical model. *Journal of Food Engineering*, 123, 36-49.

415 El Halouat, A. & Labuza, T.P. (1987) Air drying characteristics of apricots. *Journal of*
416 *Food Science*, 52, 342–345.

417 European Patent Application. (1999) Method for increasing the content of trehalose in
418 organisms through the transformation there of the cdna of the trehalose-6-
419 phosphate synthetase/phosphatase of *Selaginella Lepidophylla*. Internal publication
420 number: WO 97/42327.

421 Ferrando, M., & Spiess, W.E.J. (2001) Cellular response of plant tissue during the
422 osmotic treatment with sucrose and maltose solutions. *Journal of Food Engineering*,
423 49, 115-127.

424 Fito, P., Andrés, A., Chiralt, A., & Pardo, P. (1996) Coupling of hydrodynamic
425 mechanism and deformation–relaxation phenomena during vacuum treatments in
426 solid porous food-liquid systems. *Journal of Food Engineering*, 27, 229–240.

427 Fito, P., Chiralt, A., Betoret, N., Gras, M.L., Cháfer, M., Martínez-Monzó, J., Andrés, A.,
428 & Vidal, D. (2000) Vacuum impregnation and osmotic dehydration in matrix
429 engineering. Application in functional fresh food development. *Journal of Food*
430 *Engineering*, 49, 175-183.

431 Fito, P., LeMaguer, M., Betoret, N., Fito, & P.J. (2007) Advanced food process
432 engineering to model real foods & processes: the “safes” methodology, *Journal of*
433 *Food Engineering*, 83, 173-185.

434 Gras, M.L., Fito, P., Vidal, D., Albors, A., Chiralt, A., & Andrés, A. (2001) The effect of
435 vacuum impregnation upon some properties of vegetables. *Proceedings of the Eight*
436 *International Congress on Engineering and Food (ICEF-8)*, 260, 1361-1365.

437 Gras, M.L., Vidal, D., Betoret, N., Chiralt, A., & Fito, P. (2003) Calcium fortification of
438 vegetables by vacuum impregnation. Interactions with cellular matrix. *Journal of*
439 *Food Engineering*, 56, 279-284.

440 Hernandez, J.A., Pavon, G., & Garcia, M.A. (2000) Analytical solution of mass transfer
441 equation considering shrinkage for modeling food-drying kinetics. *Journal of Food*
442 *Engineering*, 45, 1–10.

443 Jain, N.K., & Roy, I. (2009) Effect of trehalose on proteína structure. *Protein Science*,
444 18 (1), 24-36.

445 John, M.A., & Dey, P.M. (1986) Postharvest changes in fruit cell walls, *Advances in*
446 *Food Research*, 30, 139.

447 Kowalski, S.J. (1996) Mathematical modelling of shrinkage during drying. *Drying*
448 *Technology*, 14 (2), 307–331.

449 Márquez, C.A., & De Michelis, A. (2011) Comparison of drying kinetics for small fruits
450 with and without particle shrinkage considerations. *Food and Bioprocess*
451 *Technology*, 4 (7), 1212–1218.

452 Mayor, L., & Sereno, A.M. (2004) Modelling shrinkage during convective drying of food
453 materials: a review. *Journal of Food Engineering*, 61(3), 373-386.

454 Martin, E. (2002). Utilización de microondas en el secado por aire caliente de manzana
455 (var. Granny Smith). Influencia del pretratamiento por impregnación a vacío.
456 Universitat Politècnica de Valencia. *PhD thesis*.

457 Miller, D.P., Pablo, J.J., & Corti, H. (1997) Thermophysical Properties of Trehalose and
458 Its Concentrated Aqueous Solutions. *Pharmaceutical Research*, 14 (5), 578-590.

459 Nieto, A.B., Vicente, S., Hodara, K., Castro, M.A., & Alzamora, S.M. (2013) Osmotic
460 dehydration of apple: Influence of sugar and water activity on tissue structure,
461 rheological properties and water mobility. *Journal of Food Engineering*, 119, 104-
462 114.

463 Paik, S.K., Yun, H.S., Iwahashi, H., Obucki, K., & Jin, I. (2005) Effect of trehalose on
464 stabilization of cellular components and critical targets against heat shock in
465 *Saccharomyces cerevisiae* KNU5377. *Journal of microbiology and biotechnology*,
466 15 (5), 965-970.

467 Pitt, R.E. (1992) Viscoelastic properties of fruits and vegetables. In: *Viscoelastic*
468 *properties of foods*. Rao, M.A., & Steffe, J.F. (eds), Elsevier Science, Amsterdam,
469 49-76.

470 Ratti, C. (2001) Hot air and freeze-drying of high-value foods: a review. *Journal of Food*
471 *Engineering*, 49(4), 311-319.

472 Sabarez, H.T. & Price, W.E. (1999). A diffusion model for prune dehydration. *Journal of*
473 *Food Engineering*, 42, 167–172.

474 Salvatori, D., Andrés, A., Chiralt, A., & Fito, P. (1998) The response of some properties
475 of fruits to vacuum impregnation. *Journal of Food Process Engineering*, 21, 59-73.

476 Salvatori, D., Doctorovich, R.S., & Alzamora, S.M. (2011) Impact of calcium on
477 viscoelastic properties of apple tissue. *Journal of Food Process Engineering*, 34,
478 1639-1660.

479 Segui, L., Fito, P.J., Albors, A., & Fito, P. (2006) Mass transfer phenomena during the
480 osmotic dehydration of apple isolated protoplasts (*Malus domestica* var. Fuji).
481 *Journal of Food Engineering*, 77, 179-187.

482 Senhaji, F.A., Bimbenet, J.J. & Hakam, B. (1991) Data on apricot drying: kinetics and
483 product quality. *Sciences des Aliments*, 11, 499–512.

484 Yang, H., Sakai, N., & Watanabe, M. (2001) Drying model with non-isotropic shrinkage
485 deformation undergoing simultaneous heat and mass transfer. *Drying Technology*,
486 19(1), 1441–1460.

487 Table 1. Composition of the VI solutions.
488

	Sucrose (g/L)	Trehalose dihydrated (g/L)	Calcium (g/L)
Suc	249.14	-	-
Suc+Ca	124.86	-	49.17
Tre	-	275.35	-
Tre+Ca	-	117.53	41.88

489

Table 2. Impregnation parameters values and final sugar and calcium concentrations achieved in vacuum impregnated samples (mean (standard deviation)).

	X₁	X	Y₁	Y	ε_e	X_{sugar}	X_{Ca}
Suc	-0.0221 (0.0015) ^a	0.19 (0.03) ^a	0.008 (0.009) ^a	0.02 (0.02) ^a	0.205 (0.010) ^a	0.149 (0.019)	-
Suc+Ca	-0.027 (0.007) ^a	0.192 (0.019) ^a	-0.003 (0.003) ^a	0.0159 (0.010) ^a	0.213 (0.012) ^a	0.075 (0.006)	0.029 (0.002)
Tre	-0.042 (0.012) ^a	0.17 (0.04) ^a	0 ^a	0.01 (0.02) ^a	0.208 (0.013) ^a	0.15 (0.03)	-
Tre+Ca	-0.04 (0.02) ^a	0.17 (0.05) ^a	0.020 (0.017) ^a	0.04 (0.04) ^a	0.19 (0.02) ^a	0.065 (0.015)	0.023 (0.005)

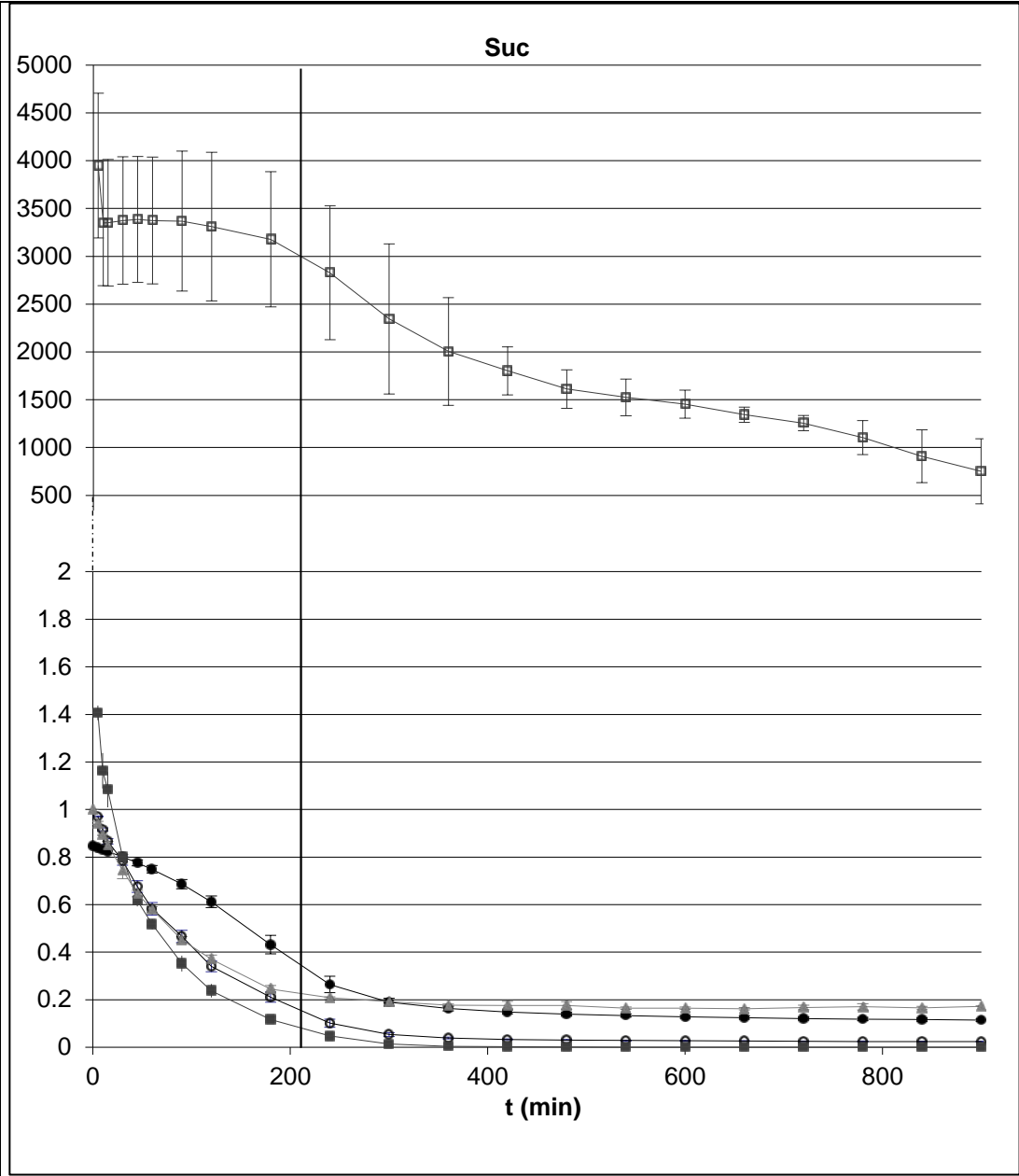
* Values with different superscript letters are significantly different (p ≤ 0.05).

490

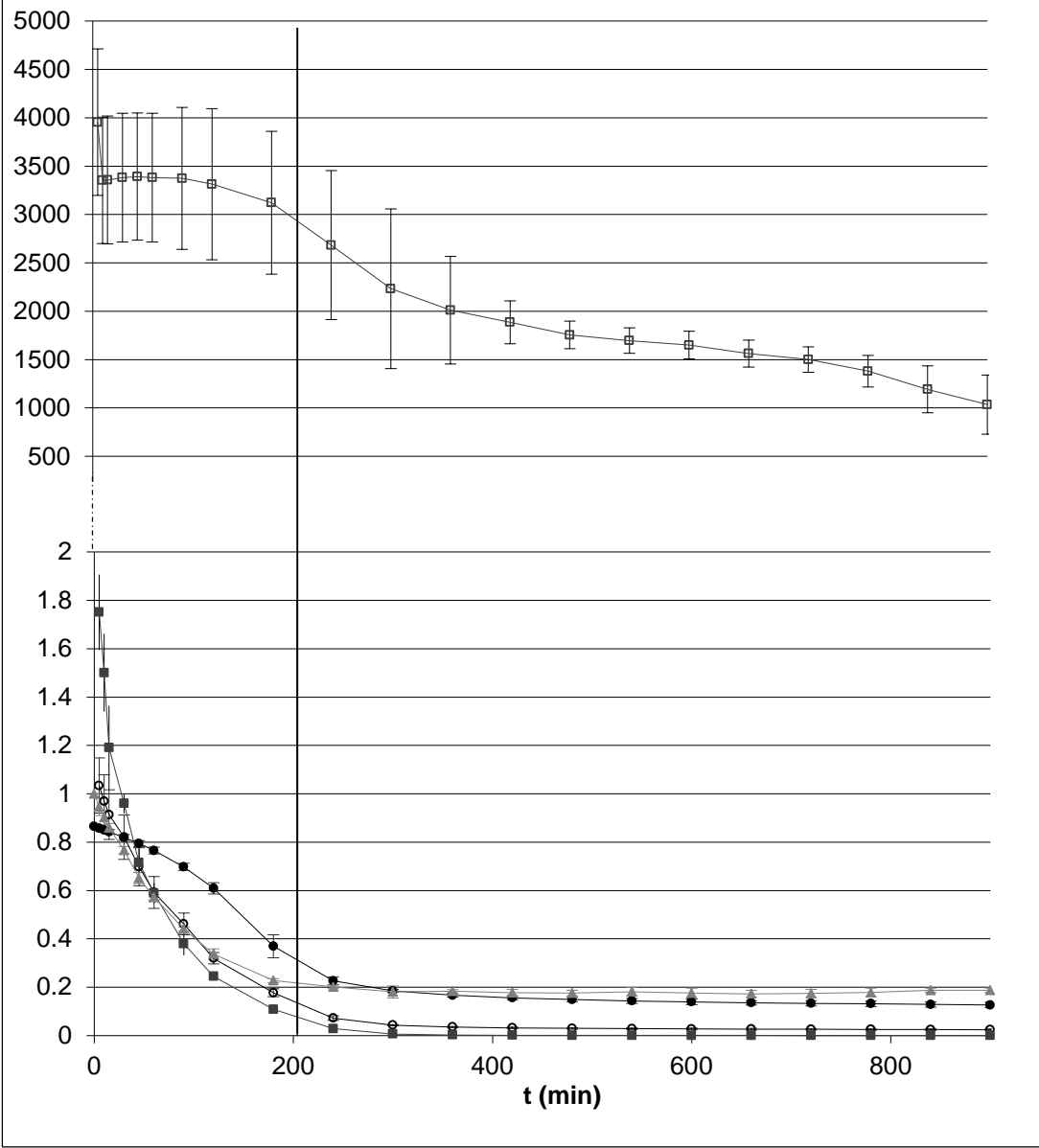
491 Table 3. Saturation times and correspondent humidities of the samples.

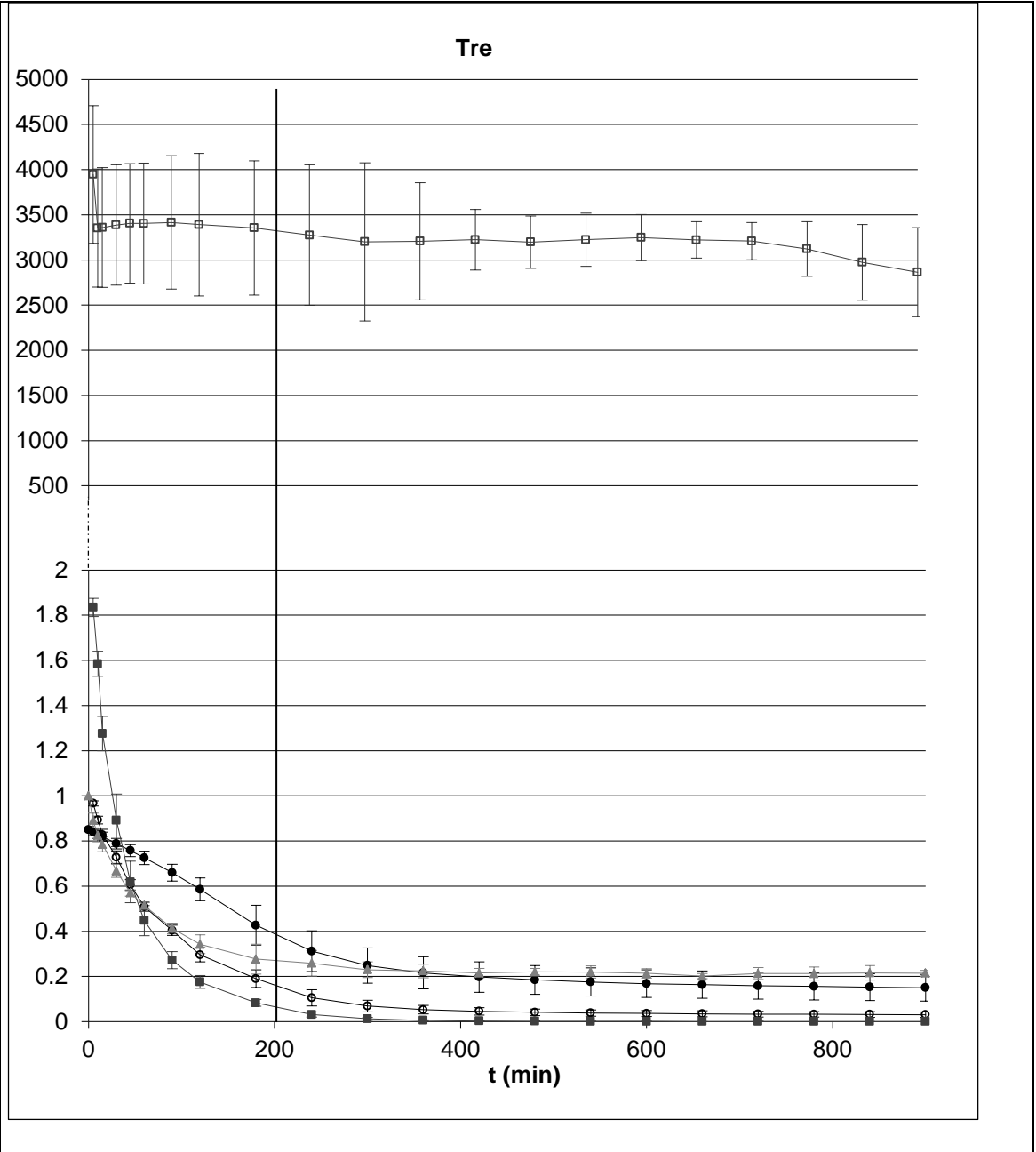
Treatment	x_w (w.b)	t_s (min.)
Suc	0.3028	211
Suc+Ca	0.3063	204
Tre	0.3431	202
Tre+Ca	0.3365	180

492



Suc+Ca





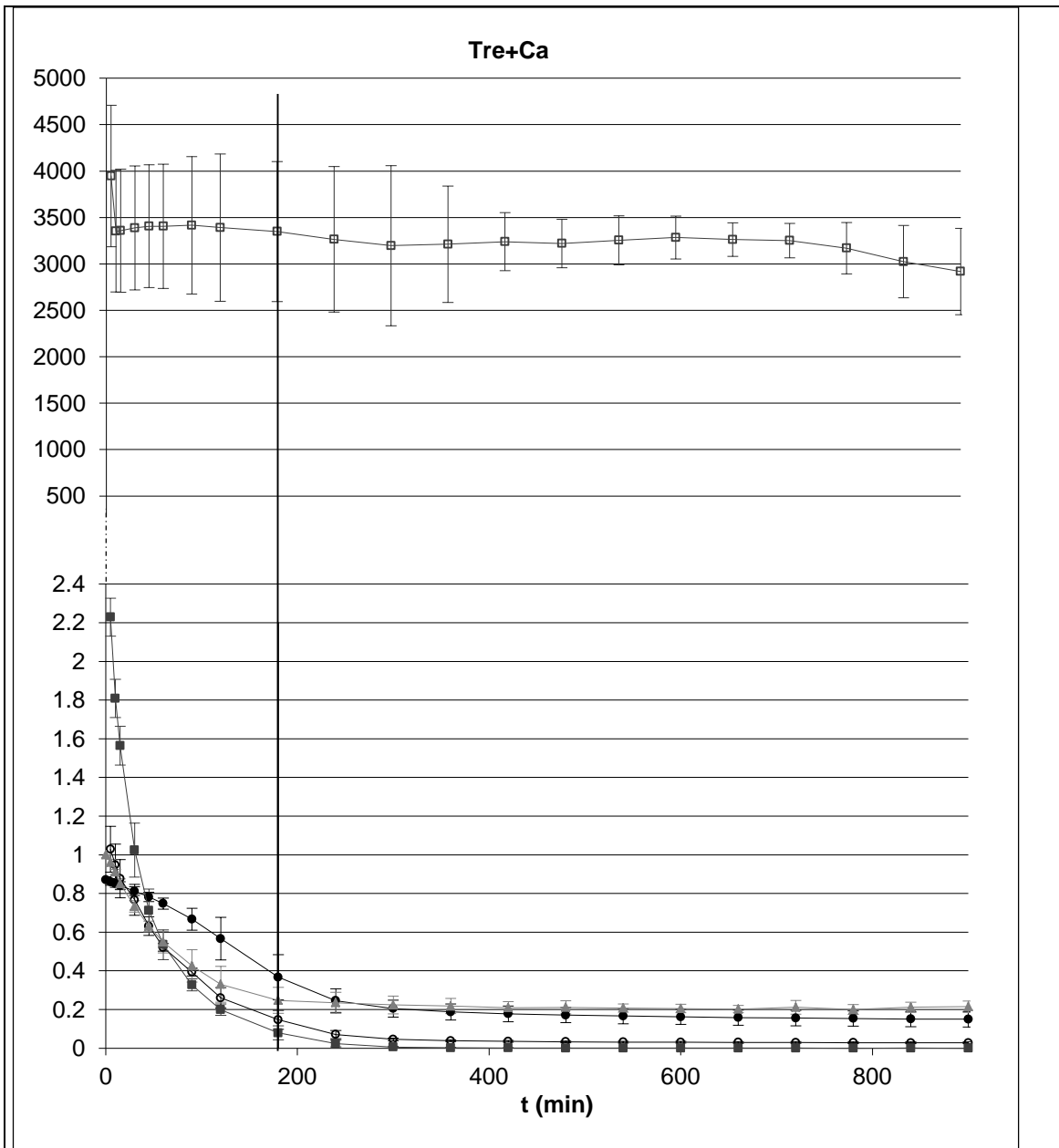


Figure 1. Representation of the humidity (w.b) ● (x_w), humidity (d.b) referred to the initial value ○ (x_w/x_{w0}), volume referred to the initial value ▲ (V/V_0), water flux ■ (J_w) ($\text{mol/m}^2\cdot\text{s}$) and chemical potential □ ($RTLn_{a_w/\varphi}$) (J/mol) of the samples dried at 40 °C versus time. Vertical line refers to the saturation time (t_s) (min).

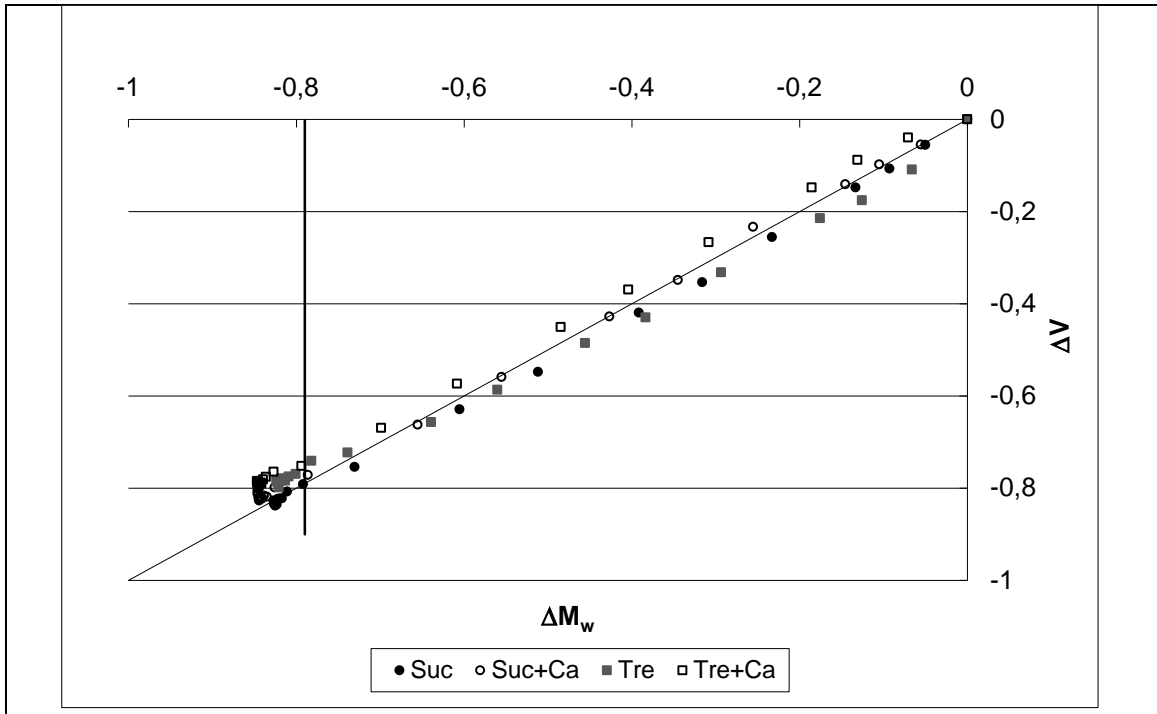


Figure 2. Variation of the total water versus total volume of the sample at 40 °C. Vertical line refers to the saturation time (t_s) (min).

494

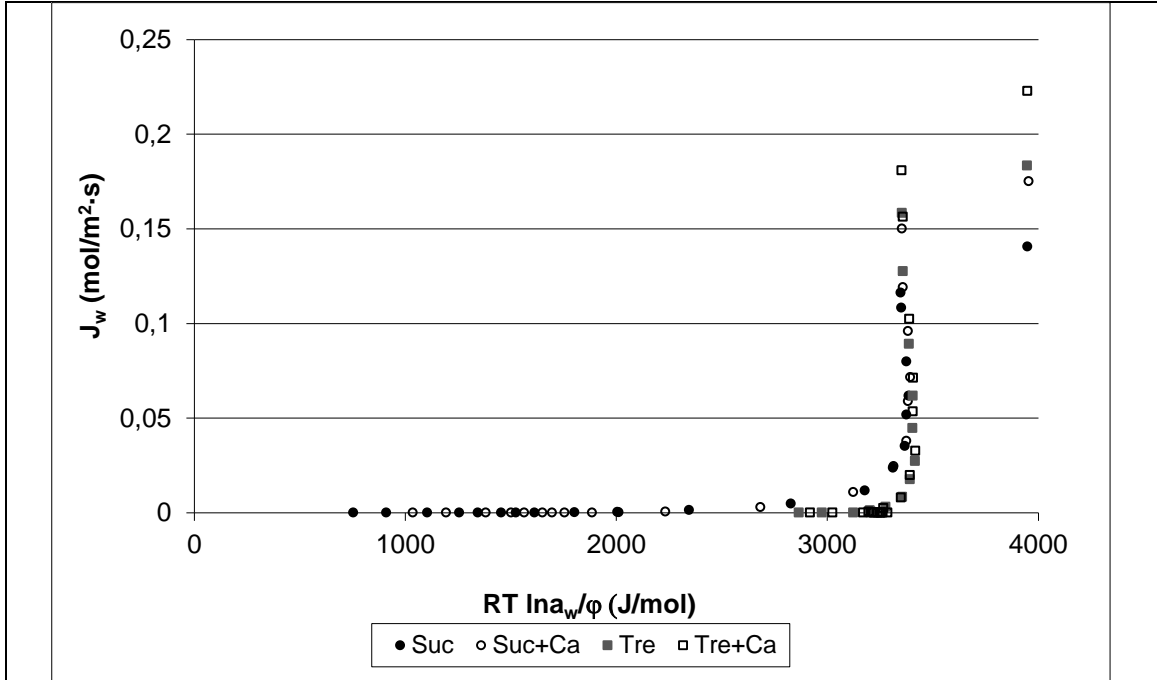
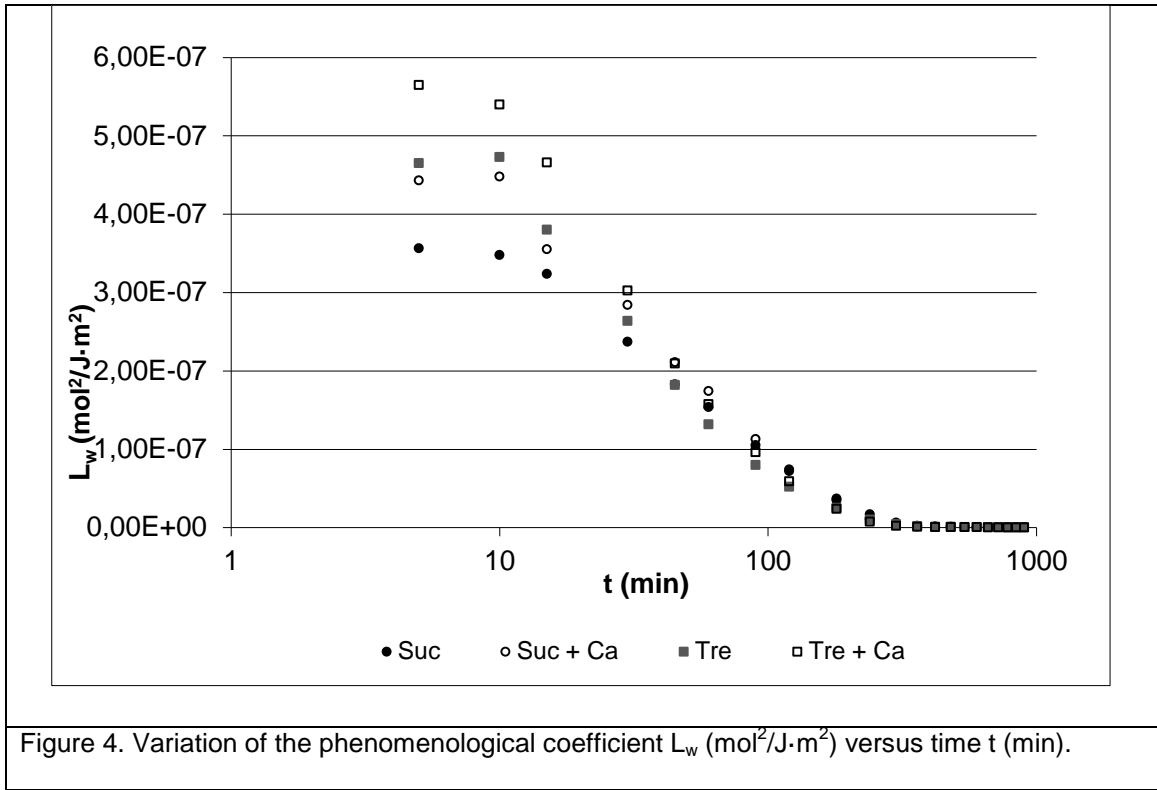
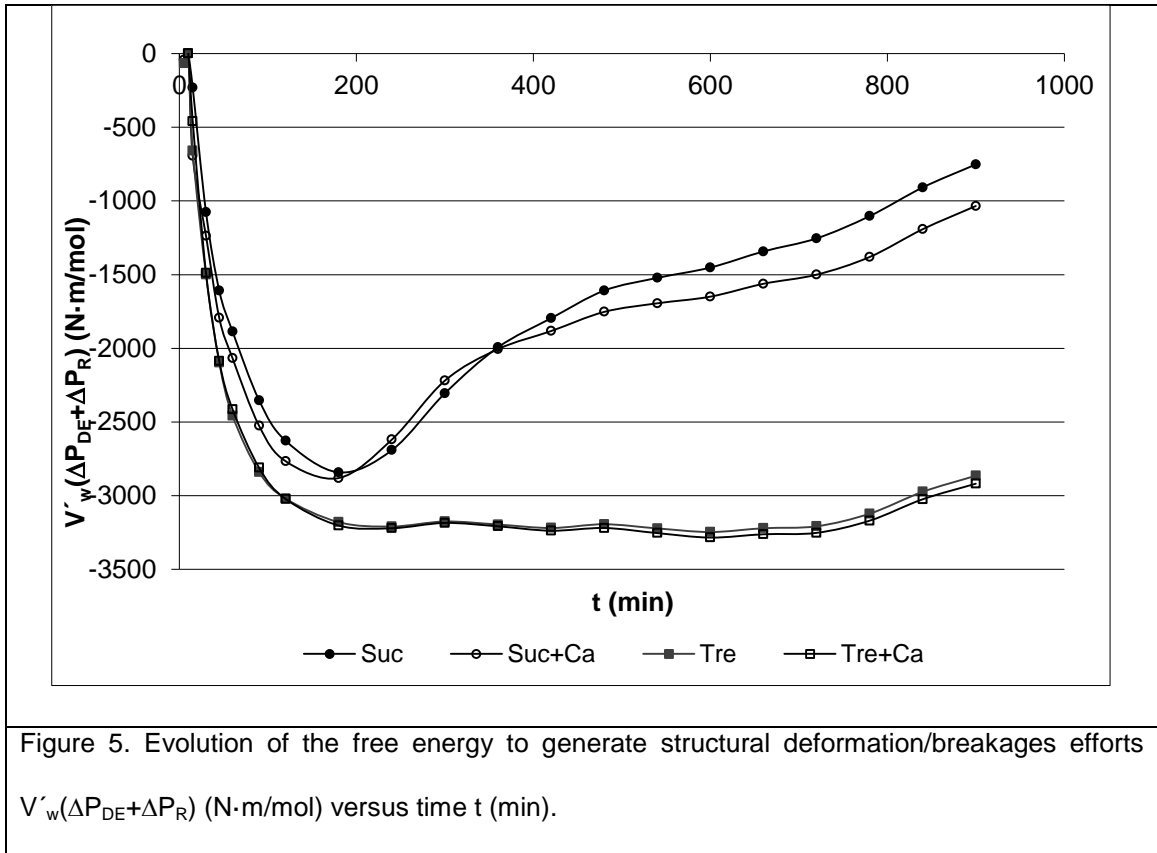


Figure 3. Variation of the water flux J_w ($\text{mol}/\text{m}^2 \cdot \text{s}$) versus driving force (J/mol).

495



496



497